ATMOSPHERIC AND OCEANIC SCIENCE LETTERS, 2012, VOL. 5, NO. 1, 43–48

Projected Changes in Asian Summer Monsoon in RCP Scenarios of CMIP5

BAO Qing

State Key Laboratory of Numerical Modeling for Atmospheric Sciences and Geophysical Fluid Dynamics (LASG), Institute of Atmospheric Physics (IAP), Chinese Academy of Sciences, Beijing 100029, China

Received 10 June 2011; revised 3 August 2011; accepted 29 August 2011; published 16 January 2012

Abstract Responses of the Asian Summer Monsoon (ASM) in future projections have been studied based on two core future projections of phase five of the Coupled Model Intercomparison Project (CMIP5) coordinated experiments with the IAP-coupled model FGOALS_s2 (the Flexible Global Ocean-Atmosphere-Land System Model). The projected changes of the ASM in climatological mean and interannual variability were respectively reported. Both the South Asian Summer Monsoon (SASM) and the East Asian Summer Monsoon (EASM) were intensified in their climatology, featuring increased monsoon precipitation and an enhanced monsoon lower-level westerly jet flow. Accordingly, the amplitude of the annual cycle of rainfall over East Asia (EA) is enhanced, thereby indicating a more abrupt monsoon onset. After the EA monsoon onset, the EASM marched farther northward in the future scenarios than in the historical runs. In the interannual variability, the leading pattern of the EASM, defined by the first multi-variable EOF analysis over EA, explains more of the total variances in the warmest future scenario, specifically, Representative Concentration Pathway (RCP8.5). Also, the correlation coefficients analysis suggests that the relationship between the EASM interannual variations and ENSO was significantly strengthened in the future projections, which may indicate improved predictability of the EASM interannual variations.

Keywords: Asian Summer Monsoon, CMIP, ENSO, monsoon change, FGOALS, EASM

Citation: Bao, Q., 2012: Projected changes in Asian Summer Monsoons in RCP scenarios of CMIP5, *Atmos. Oceanic Sci. Lett.*, **5**, 43–48.

1 Introduction

The Asian summer monsoon (ASM) is the strongest summer monsoon system in the world, and more than half of the world's population inhabits the region of the ASM. The agriculture, economy, and society across the ASM regions are critically influenced by the intensity, evolution, and variation of the ASM. Therefore, studying how the ASM will change in the future is imperative. Climate system models have become a useful tool to simulate past climate and project the future changes of climate. Therefore, it is necessary to use a climate system model to investigate the change of the ASM in the future.

Previous studies have investigated the responses of the climatology of the ASM to global warming. The earliest numerical study was made with the National Center for Atmospheric Research (NCAR) model, which showed that the South Asian Summer Monsoon (SASM) would become stronger in future projections, due to the increased land-sea thermal contrast between the Eurasian continent and the Indian Ocean (Meehl and Washington, 1993). Other studies with different models have also shown that the precipitation of the SASM will increase in the future (Bhaskaran et al., 1995; Kitoh, 2006; Sabade et al., 2011). Several studies have also reported the changes of the East Asian Summer Monsoon (EASM) in future climate projections (Kitoh, 2006; Kripalani et al., 2007; Zhao et al., 2008). Using the multi-model ensemble technique, Kripalani et al. (2007) showed that the summer precipitation increased from 5% to 10% over East Asia, due to the intensification of the projected Western Pacific Subtropical High (WPSH). Furthermore, Sun and Ding (2010) revealed that the enhanced precipitation of the EASM is the result of the change of both the monsoon circulation and water vapor. Regarding the projected changes of seasonal monsoon evolution, Kitoh (2006) documented an early onset of the monsoon rainy season and the postponement of the monsoon's withdrawal.

Several studies been conducted on the projected changes of the interannual variations of the ASM, and a number of studies have studied the projected change of the relationship between the ASM and ENSO. Annamalai et al. (2007) and Sabade et al. (2011) found no significant changes of the relationship between SASM and ENSO in the future. Observations have shown that the relationship between the EASM and ENSO has strengthened during the past three decades (Wang et al., 2008; Kim et al., 2008). How the relationship between the EASM and ENSO changes remains unanswered.

With the latest version of the Institute of Atmospheric Physics (IAP) atmosphere-land-ocean coupled climate system model, the future projections of a new coordinated climate model experiment, known as CMIP5 (the fifth experiment of the Coupled Model Intercomparison Project, which will be used for the Intergovernmental Panel on Climate Change (IPCC) fifth assessment report), have been proposed. The future projections are called RCP experiments, that is, Representative Concentration Pathway scenarios (Taylor et al., 2009). Results from both RCP4.5 and RCP8.5 are available to diagnose the changes of the ASM ('4.5' or '8.5' identifies a concentration pathway that approximately results in a radiative forcing

Corresponding author: BAO Qing, baoqing@mail.iap.ac.cn

of 4.5 or 8.5 W m^{-2} at the year 2100, relative to pre-industrial conditions (year 1850) (Taylor et al., 2009)).

In this work, we attempt to use the CMIP5 outputs from the IAP coupled model to answer the following question: what are the changes of the ASM in the future scenarios of RCP4.5 and RCP8.5 in its climatology, interannual variations, and relationship with ENSO? The second section provides a description of the IAP coupled climate system model and the CMIP5 experimental designs. The datasets and methodology are introduced in section 3, and section 4 shows the results from the model's projections (RCP4.5 and RCP8.5). The discussion and conclusions are given in the final section.

2 Model and experimental design

The IAP climate system model used in this study is the second spectral version of the Flexible Global Ocean-Atmosphere-Land System model (FGOALS_s2). This model provides state-of-the-art computer simulations of the Earth's past, present, and future climate states (Zhou et al., 2005; Bao et al., 2010). The atmospheric component is the Spectral Atmospheric Model of the IAP/State Key Laboratory of Numerical Modeling for Atmospheric Sciences and Geophysical Fluid Dynamics (LASG) (SAMIL) (Wu et al., 1996, 2004; Wang et al., 2005; Bao et al., 2006, 2010). The horizontal resolution is 2.81°/1.66° longitude/latitude with 26 hybrid vertical layers. The oceanic component is the LASG IAP Common Ocean Model (LICOM) (Liu et al., 2004), and its resolution is one degree by one degree with an increased resolution to half a degree by half a degree in the tropical regions. The other components, including land surface, ice, and coupler components, are from the NCAR Community Climate System Model (CCSM) (Kiehl and Gent, 2004).

To investigate the projected changes of the ASM, the results from three groups of CMIP5 coordinated experiments with FGOALS_s2 have been taken, including the historical simulations and the RCP4.5 and RCP8.5 future projections. The historical simulations have been integrated from 1850 to 2005, and both RCP4.5 and RCP8.5 have been projected from 2006 to 2100. The imposed changing conditions of the historical simulations and future projections include atmospheric composition (including CO_2) due to anthropogenic and volcanic influences, solar forcing, and concentrations of short-lived species and natural and anthropogenic aerosols. These experiments are all standard runs based on the CMIP5 experimental design (Taylor et al., 2009). To reduce the uncertainties arising from differing initial conditions, the historical simulations and RCP projections have three individual ensemble members, which are achieved with the different initial conditions derived from the pre-industry experiment. The follow evaluations and diagnoses were retrieved from these three ensemble methods.

3 Datasets and methodology

The datasets used to evaluate the model include the reanalysis circulation fields from the National Centers for Environmental Prediction(NCEP)-NCAR (Kalnay et al., 1996); precipitation from the Global Precipitation Climatology Project (GPCP) (Xie et al., 2003); and the SST dataset from the Hadley Centre of the UK Meteorological Office (HadISST) (Rayner et al., 2003). To be consistent with the model, all of the datasets have been gridded to a 2.81°/1.66° longitude/latitude resolution.

To obtain the leading pattern of the EASM interannual variability (IAV), a Multi-Variate EOF analysis (MV-EOF) was applied (Liu et al., 2008). The four variables selected for MV-EOF include observed precipitation, sea-level pressure, 850 hPa zonal winds, and 850 hPa meridional winds. The MV-EOF analysis method has been described in detail by Wang (1992). This method has the advantage of capturing spatial phase relationships among various selected circulation and precipitation fields. In the MV-EOF analysis, an area-weighted, normalized covariance matrix was constructed for the combined four meteorological fields. After the EOF decomposition, dimensional eigenvectors (spatial patterns) are obtained and presented.

4 Results from the numerical experiments

Before showing the projected changes of the ASM, the general performance of FGOALS_s2 have been presented through comparisons between the observations and historical simulations. Figure 1 is the climatological ASM in the observation, the historical simulation and the future projection. The vectors are the lower-level wind (850 hPa) and the shading stands for rainfall. As illustrated in Figs. 1a (observations) and 1b (historical simulations), FGOALS_s2 realistically reproduces the South Asian monsoon circulation, including the cross-equatorial low-level jet (namely, the Somali Jet) and two monsoon troughs: one trough located to the east of the Arabian Peninsula and the other trough located over the South China Sea. Compared with the GPCP (Fig. 1a) observation, the locations of these three monsoon rainfall centers have been well simulated in the historical simulations.

Figures 1d and 1f show the differences between the RCP4.5/RCP8.5 projections and the historical simulations, which exhibit the projected changes of the climatological ASM. Although the future emission scenarios have been updated in CMIP5 (Taylor et al., 2009), it is shown that the SASM becomes intensified (Figs. 1c–f), which is consistent with previous projections (Meehl and Washington, 1993; Annamalai et al., 2007; Sabade et al., 2011). The strengthened monsoon systems are featured with increased monsoon precipitation and an enhanced monsoon lower-level westerly jet flow. Over the EA regions, the precipitation increases along the EA subtropical front in both the RCP4.5 and RCP8.5 projections, which are associated with the strengthened WPSH (Figs. 1c–f).

The projected changes of the EASM are not only restricted to the climatological mean precipitation and monsoon flow but also include the monsoon seasonality. The annual cycle of rainfall over the EA regions (averaged from 110°E to 120°E) is shown in Fig. 2, and this cycle illustrates the seasonal march and retreat of the EA rainfall related with the seasonality of the EA monsoon

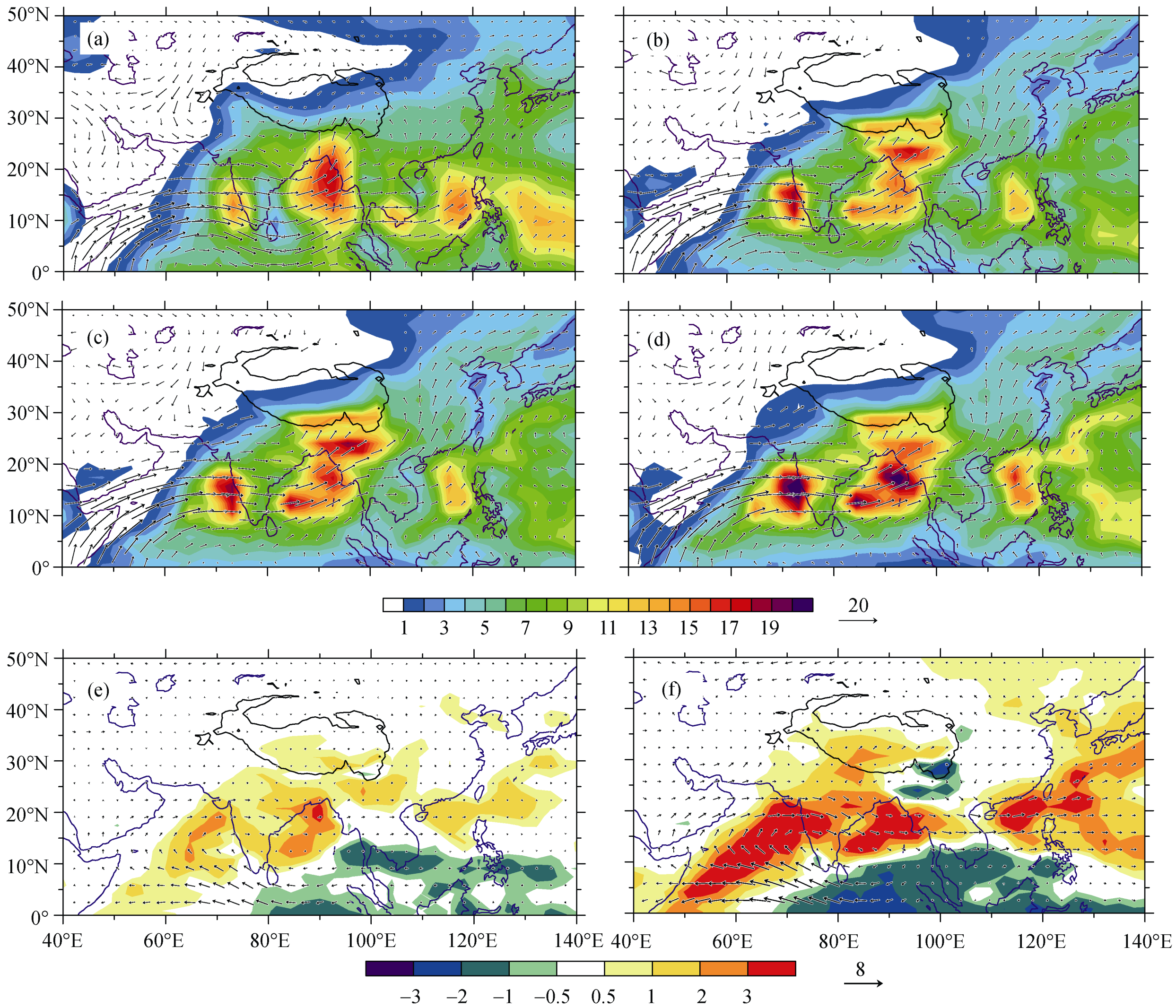

Figure 1 Climatological summer (JJA) mean precipitation (color shading in mm d^{-1}) and 850 hPa winds (vectors in units of m s^{-1}) in (a) observation (wind is from NCEP reanalysis and precipitation from CMAP datasets); (b) CMIP5-historical (1986–2005); (c) CMIP5-RCP4.5 (2081–2100), (d) CMIP5-RCP8.5 (2081–2100); (e) the differences between RCP4.5 and the historical runs; (f) the differences between RCP8.5 and the historical runs.

circulations. Compared with the rainfall march derived from GPCP, FGOALS_s2 can reasonably capture the dry and wet phases of the East Asian monsoon in historical simulations (Figs. 2a and 2b): the clearly persistent rainfall beginning in the middle of February is presented in the model's results (namely, the EA Spring Persistent Rainfall (Wu et al., 2007)), and the northward march of the monsoon rainfall is also well reproduced with the movement of the solar position; these results are consistent with the prior observation.

As illustrated in Figs. 2c–f, the projected changes of the monsoon seasonality include the amplitude of the EA monsoon annual cycle and the march of the EASM: although there is no significant change of the EASM onset time, the features of its onset becomes obvious because there are negative precipitation anomalies in the pre-monsoon but the positive precipitation anomalies occur after monsoon onset; also, after the EA monsoon onset, the EASM march becomes more northward, especially in the RCP8.5 projections (Figs. 2d and 2f). The changes of the monsoon's withdrawal are quite different between the RCP4.5 and RCP8.5 scenarios. The withdrawal of the monsoon is earlier in RCP4.5, with a negative precipitation anomaly after September, but it appears later in RCP8.5, being characterized with a positive precipitation anomaly after September (Figs. 2e and 2f).

Figure 3 shows the observed, simulated, and projected leading patterns of the EASM. The first leading mode of the simulated EASM in the historical run (Fig. 3b) is characterized by a prominent abnormal West Pacific Subtropical High (WPSH). As addressed in Bao et al. (2010), the model biases are mainly the northward shifting of the north boundary of the Western North Pacific (WNP) subtropical high, which is associated with a negative precipitation belt over the Middle-lower Yangtze River, the Korean Peninsula, and the northern parts of Japan.

The projections of EASM IAV have also demonstrated notable changes. Compared with the historical simulations and RCP projections, the total variation of the IAV of the EASM has distinctly increased from 46.6% to 56.9% in the RCP8.5 scenario, which means that the IAV of the EASM becomes more dominant with a high green-

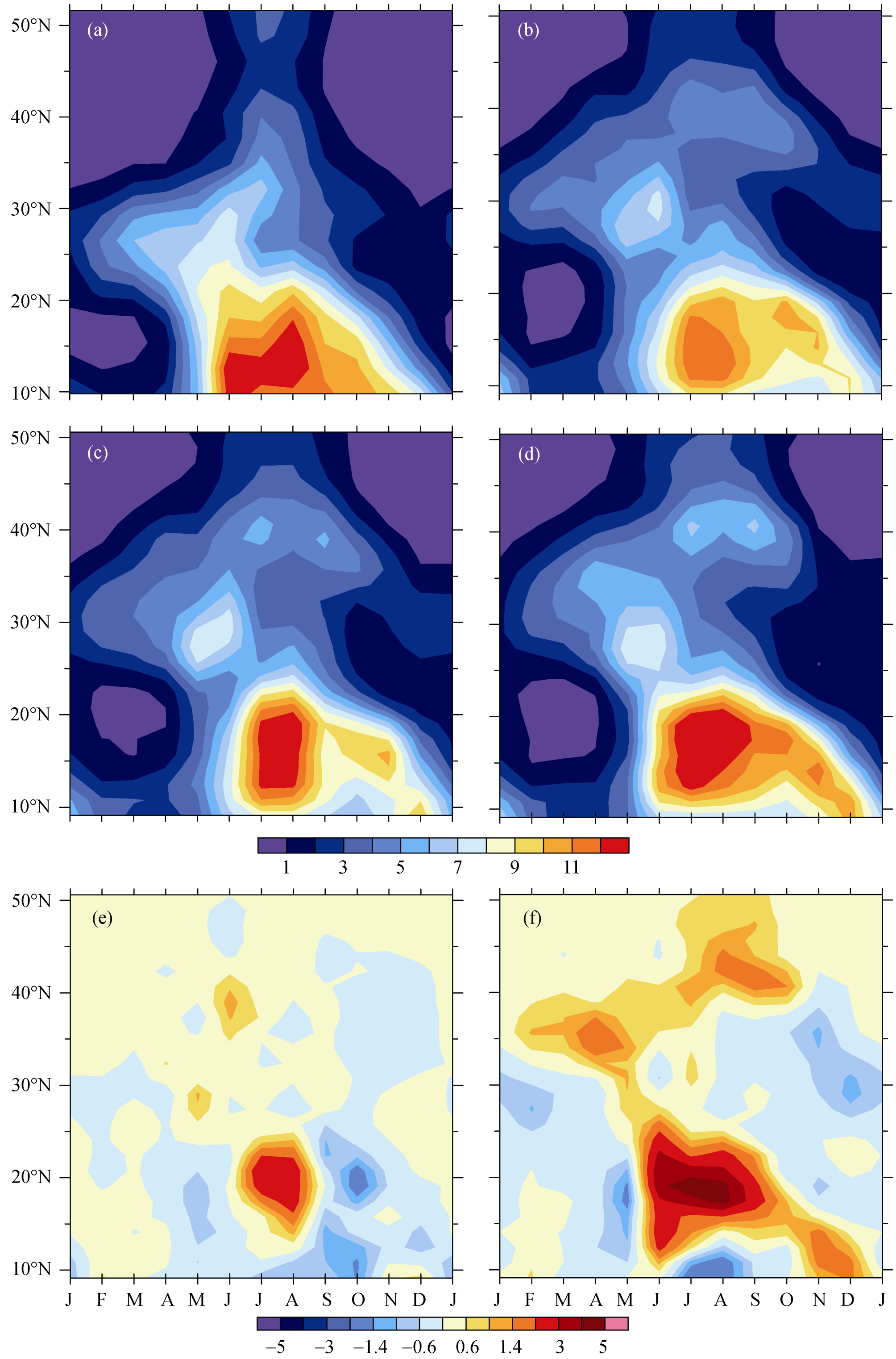

Figure 2 Climatological annual cycle of 110–120°E zonal mean precipitation (mm d^{-1}) in (a) GPCP; (b) CMIP5-historical (1986–2005); (c) CMIP5-RCP4.5 (2081–2100), (d) CMIP5-RCP8.5 (2081–2100); (e) the differences between RCP4.5 and the historical runs; (f) the differences between RCP8.5 and historical simulations.

house emission scenario. Figure 4 presents the correlation coefficients between the time series of the EASM leading pattern and the Niño3.4 index. The Niño3.4 index is defined as the average of the sea surface temperature anomalies over the region between 5°N–5°S and 170–120°W. As shown in Fig. 4, the correlation coefficients in the projections increase from the historical simulations to the future projections, and the increased correlation coefficients indicate that the relationship between the EASM IAV and ENSO have been significantly strengthened. This strengthened relationship potentially indicates an increase of the predictability of the EASM interannual variations.

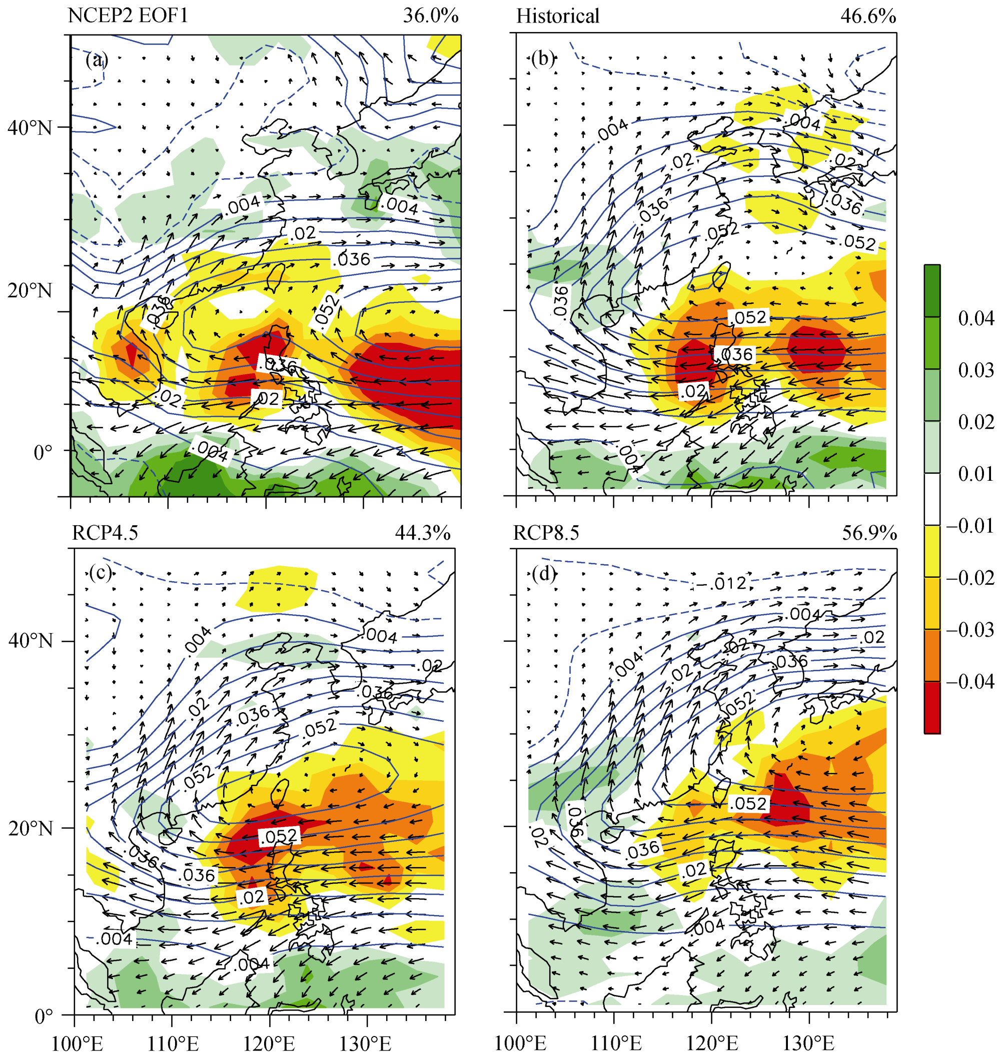

Figure 3 The spatial patterns of the first MV-EOF mode of the EASM. All panels are 850 hPa winds (vectors in units of m s^{-1}), precipitation (color shading in units of mm d^{-1}), and sea-level pressure (contours in units of hPa). (a) Observations, (b) CMIP5-historical, (c) CMIP5-RCP4.5, and (d) CMIP5-RCP8.5.

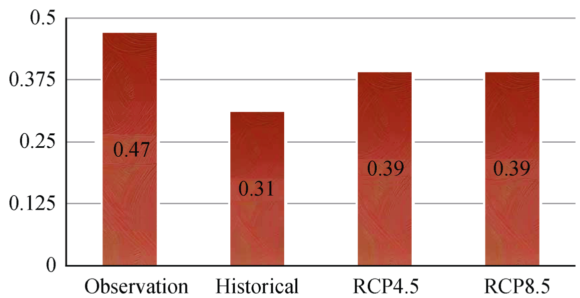

Figure 4 The correlation coefficients between the time series of the leading pattern of the EASM and the Niño3.4 index in the observation, CMIP5-historical, CMIP5-RCP4.5, and CMIP5-RCP8.5.

5 Discussion and conclusions

The future projected changes of the ASM have been studied based on CMIP5 coordinated experiments with the IAP-coupled model FGOALS_s2. The changes in climatology, seasonality, and interannual variations have been reported. Based on historical simulations and RCP4.5/ RCP8.5 projections, the projected results indicate that both the SASM and the EASM become clearly strengthened: the monsoon precipitation has been increased, and the monsoon lower-level westerly jet flow has been enhanced, which are results that are consist with previous studies (Meehl and Washington, 1993; Bhaskaran et al., 1995; Kitoh, 2006; Sabade et al., 2011); accordingly, the EA annual cycle of precipitation becomes enhanced, which indicates a more abrupt monsoon, while after the EA monsoon onset, the EASM marches more northward in the future scenarios compared with the current simulations in the historical runs. In addition, based on the CMIP5 future scenarios, the changes of the EASM IAV were first discussed in this study: the EASM leading pattern, which is defined by the first multi-variable EOF analysis over EA, explains more total variances in the warmest future scenario, RCP8.5, and the correlation coefficients analysis suggests that the relationship between the EASM interannual variations and ENSO has been significantly strengthened. This strengthened relationship may indicate the improved predictability of the EASM interannual variations.

Acknowledgements. I thank Mr. WANG Jun for performing the MV-EOF analysis and the two anonymous reviewers for their valuable suggestions. This research is supported by the Chinese Academy of Sciences (XDA05110303), the National Basic Research Program of China (973 Program, 2012CB417203), and the National Natural Science Foundation of China (40805038 and 41023002).

References

Annamalai, H., K. Hamilton, and K. Sperber, 2007: South Asian summer monsoon and relationship with ENSO in the IPCC AR4 simulations, *J. Climate*, **20**, 1071–1092.

Bao, Q., Y. M. Liu, T. J. Zhou, et al., 2006: The sensitivity of the Spectral Atmospheric General Circulation Model of LASG/IAP to the land process, *Chinese J. Atmos. Sci.*, **30**, 1077–1090.

Bao, Q., G. Wu, Y. Liu, et al., 2010: An introduction to the coupled model FGOALS1.1-s and its performance in East Asia, *Adv. Atmos. Sci.*, **27**(5), 1131–1142.

Bhaskaran, B., J. F. B. Mitchell, J. R. Lavery, et al., 1995: Climatic response of the Indian subcontinent to doubled CO_2 concentrations, *Int. J. Climatol.*, **15**(8), 873–892.

Kalnay, E., M. Kanamitsu, R. Kistler, et al., 1996: The NCEP/NCAR 40-year reanalysis project, *Bull. Amer. Meteor. Soc.*, **77**, 437–471.

Kiehl, J. T., and P. R. Gent, 2004: The Community Climate System Model, Version 2, *J. Climate*, **17**, 3666–3682.

Kim, H.-J., B. Wang, and Q. Ding, 2008: The global monsoon variability simulated by CMIP3 Coupled Climate Models, *J. Climate*, **21**, 5271–5294.

Kitoh, A., 2006: Asian monsoons in future, in: *The Asian Monsoon*, B. Wang (Ed.), Praxis Publishing, New York, 631–649.

Kripalani, R. H., J. H. Oh, and H. S. Chaudhari, 2007: Response of the East Asian summer monsoon to doubled atmospheric CO_2: Coupled Climate Models simulations and projections under IPCC AR4, *Theor. Appl. Climatol.*, **87**, 1–28.

Liu, H. L., X. H. Zhang, W. Li, et al., 2004: An eddy-permitting oceanic general circulation model and its preliminary evaluations, *Adv. Atmos. Sci.*, **21**, 675–690.

Liu, J., B. Wang, and J. Yang, 2008: Forced and internal modes of variability of the East Asian summer monsoon, *Climate Past Discuss.*, **4**, 645–666.

Meehl, G. A., and W. M. Washington, 1993: South Asian summer monsoon variability in a model with doubled atmospheric carbon dioxide concentration, *Science*, **260**, 1101–1104.

Rayner, N. A., D. E. Parker, E. B. Horton, et al., 2003: Global analyses of sea surface temperature, sea ice, and night marine air temperature since the late nineteenth century, *J. Geophys. Res.*, **108**(D14), 4407, doi:10.1029/2002JD002670.

Sabade, S. S., A. Kulkarni, and R. H. Kripalani, 2011: Projected changes in South Asian summer monsoon by multi-model global warming experiments, *Theor. Appl. Climatol.*, **103**, 543–565.

Sun, Y., and Y. H. Ding, 2010: A projection of future changes in summer precipitation and monsoon in East Asia, *Sci. China Ser. D-Earth Sci.*, **53**, 284–300.

Taylor, K. E., R. J. Stouffer, and G. A. Meehl, 2009: *A Summary of the CMIP5 Experiment Design*, available at http://cmip-pcmdi.llnl.gov/cmip5/experiment_design.html, 33pp.

Wang, B., 1992: The vertical structure and development of the ENSO anomaly mode during 1979–1989, *J. Atmos. Sci.*, **49**(8), 698–712.

Wang, B., J. Yang, T. Zhou, et al., 2008: Interdecadal changes in the major modes of Asian-Australian monsoon variability: Strengthening relationship with ENSO since the late 1970s, *J. Climate*, **21**, 1771–1789, doi:10.1175/2007JCLI1981.1.

Wang, Z.-Z., G.-X. Wu, P. Liu, et al., 2005: The development of GOALS/LASG AGCM and its global climatological features in climate simulation. I: Influence of horizontal resolution, *J. Tropical Meteor.*, **21**, 225–237.

Wu, G., H. Liu, Y.-C. Zhao, et al., 1996: A nine-layer atmospheric general circulation model and its performance, *Adv. Atmos. Sci.*, **13**(1), 1–18.

Wu, G., Y. Liu, T. Wang, et al., 2007: The influence of mechanical and thermal forcing by the Tibetan Plateau on Asian climate, *J. Hydrometeor.*, **8**, 770–789.

Wu, T., Z. Wang, Y. Liu, et al., 2004: An evaluation of the effects of cloud parameterization in the R42L9 GCM, *Adv. Atmos. Sci.*, **21**, 153–162.

Xie, P. P., J. E. Janowiak, P. A. Arkin, et al., 2003: GPCP pentad precipitation analyses: An experimental dataset based on gauge observations and satellite estimates, *J. Climate*, **16**, 2197–2214.

Zhao, Z., A. Kitoh, and D.-K. Lee, 2008: Warming in East Asia as a consequence of increasing greenhouse gases, in: *Changes in the Human-Monsoon System of East Asia in the Context of Global Change*, C. Fu et al. (Eds.), World Scientific Publishing Co., Singapore, 105–114.

Zhou, T., R. Yu, Z. Wang, et al., 2005: *Atmospheric Circulation Global Model (SAMIL) and the Coupled Model (FGOALS-s)* (in Chinese), China Meteorological Press, Beijing, 288pp.